以 Lid-Driven Cavity 流場比較平行晶格波茲曼 SRT 與 MRT 法

Assessment of SRT and MRT Scheme in Parallel Lattice Boltzmann Method for Lid-Driven Cavity Flows

J.-S. Wu

Y.-L. Shao

Department of Mechanical Engineering
National Chiao-Tung University

Abstract

Two-dimensional near-incompressible steady lid-driven cavity flows (Re=100-7,500) are simulated using multi-relaxation-time (MRT) model in the parallel lattice Boltzmann BGK method (LBGK). Results are compared with those using single-relaxation-time (SRT) model in the LBGK method and previous simulation data using Navier-Stokes equations for the same flow conditions. Effects of variation of relaxation parameters in the MRT model, effects of number of the lattice points, improved computational convergence and reduced spatial oscillations of solution near geometrically singular points in the flow field using LBGK method due to MRT model are highlighted in the study. In summary, lattice Boltzmann method using MRT model introduces much less spatial oscillations near geometrical singular points, which is important for the successful simulation of higher Reynolds number flows.

Keywords: Lattice Boltzmann BGK method, Multi-relaxation-time, Single-relaxation-time

I. INTRODUCTION

The lattice Boltzmann equation (LBE) using relaxation technique was introduced by Higuerea and Jimenez [1] to overcome some drawbacks of lattice gas automata (LGA) such as large statistical noise, limited range of physical parameters, non-Galilean invariance, and implementation difficulty in three-dimension problem. In the original derivation of LBE using relaxation concept, it was strongly connected to the underlying LGA. But it was soon recognized that it could be constructed independently [2]. Since then, the lattice Boltzmann methods (LBM) have received considerable attention as an alternative to traditional computational fluid dynamics for simulating certain complex flow problems. The simplest LBE is the lattice Bhatnager-Gross-Krook (LBGK) equation [3], based on a single-relaxation-time (SRT) approximation. Due to the extreme simplicity, the lattice BGK (LBGK) equation [4] has become the most popular lattice Boltzmann model in spite of its deficiencies, for example, in simulating high-Reynolds numbers flow.

In the LBM, fluid is modeled by particles moving on a regular lattice. At each time step particles propagate to neighboring lattice sites and re-distribute their velocities in a local collision phase. The inherent locality of the scheme makes it perfect for parallel computing [5], whose advantage will be taken in the current

study. Through Chapman-Enskog multi-scale expansion [6], the complicated, nonlinear compressible Navier-Stokes equations can be recovered from the simple, linear LBGK equation based on the assumptions that, first, Mach number is small, and, second, the density varies slowly in the flow field. Thus, the LBM has been applied mostly to compute the flow field in near-incompressible limit. In particular, the LBGK method has been successfully applied to problems of near-incompressible flows through porous media [7], multiphase flows [8] and dynamics of droplet breakup [9], to name a few.

However, there exist some deficiencies in solving higher Reynolds number incompressible flow problems or resolving flow fields near geometrically singular points using single-relaxation-time (SRT) LBM [10,11]. On one hand, the fluid density is required to be nearly constant for nearly incompressible flows and the pressure is proportional to the local density field. On the other hand, pressure and shear stress are singular near the geometrically singular points (e.g., sharp corners). Hence, it often causes unphysical, strong local spatial oscillations near these singular points, which turns out to contaminate the flow field far away from these singular points. Previous work originally developed by D'Humieres [11], and further extended by Lallemand and Luo [12] suggests that the use of a multi-relaxation-time (MRT) model can improve the numerical stability and reduce dramatically the unphysical oscillations for some simple flows. They concluded that using MRT model in the LBM in these simple flows can significantly reduce the spatial oscillation near the singular points and improves the quality of the solution at higher Reynolds number. However, there is no systematic study in revealing the limits of applying the MRT model in the LBM for higher Reynolds number flows, which have complicated flow features.

II. NUMERICAL METHOD

II.1 Lattice Boltzmann Method with SRT model

LBM method solves the microscopic kinetic equation for particle distribution *f(x,v,t)*, where *x* and *v* is the particle position and velocity vector, respectively, in phase space *(x,v)* and time *t*, where the macroscopic quantities (velocity and density) are obtained through moment integration of *f(x,v,t)*. The most popular used LBM equation is the single-relaxation-time LBGK model [4], and listed as follows,

$$f_i(\bar{x}+\bar{e}\Delta t, t+\Delta t) - f_i(\bar{x},t) = -\omega[f_i(\bar{x},t) - f_i^{eq}(\bar{x},t)] \quad (1)$$

where $f_i(\bar{x},t)$ and $f_i^{eq}(\bar{x},t)$ are the particle distribution function and the equilibrium particle distribution function of the *i*-th discrete particle velocity v_i, respectively, $\bar{e}$ is a discrete velocity vector and $\omega = \frac{\Delta t}{\tau}$ is the collision frequency. Note that τ is the collision relaxation time.

The 9-velocity LBE model on the 2-D square lattice (Fig. 1), denoted as the D2Q9 model, is used in the current study for simulating the steady lid-driven cavity flow. For isothermal near-incompressible flows, the equilibrium distribution function can be derived as the following form [6]:

$$f_i^{eq}(\bar{x},t) = \rho w_i[1 + \frac{3}{c^2}\bar{e}_i\cdot\bar{u} + \frac{9}{2c^4}(\bar{e}_i\cdot\bar{u})^2 - \frac{3}{2c^2}\bar{u}\cdot\bar{u}] \quad (2)$$

where w_i is a weighting factor, $\bar{u}$ is the fluid velocity and $c = \frac{\Delta x}{\Delta t} = \frac{\Delta y}{\Delta t}$, for square lattice, is the lattice streaming speed, and Δx, Δy and Δt are the lattice width, height and advancing time step, respectively. In addition, the discrete velocities for D2Q9 model are

$$\bar{e}_i = \begin{cases} (0,0) & i = 0, \textit{rest particle} \\ (\pm c,0),(0,\pm c) & i = 1,2,3,4 \\ (\pm c,\pm c) & i = 5,6,7,8 \end{cases} \quad (3)$$

and the values of the weighting factors w_i are

$$w_i = \begin{cases} 4/9 & i = 0, \textit{rest particle} \\ 1/9 & i = 1,2,3,4 \\ 1/36 & i = 5,6,7,8 \end{cases} \quad (4)$$

The density and velocities can be computed simply by moment integration as

$$\rho = \sum_i f_i = \sum_i f_i^{eq} \quad (5)$$

$$\bar{u} = \frac{1}{\rho}\sum_i \bar{e}_i f_i = \frac{1}{\rho}\sum_i \bar{e}_i f_i^{eq} \quad (6)$$

Application of the multi-scale technique (Chapman-Enskog expansion) yields the Navier-Stokes equation with the pressure $p = \rho c_s^2$, where $c_s = \frac{c}{\sqrt{3}}$, and an advection term with Galilean invariance. The viscosity of the simulated fluid is $\nu = \Delta t(\frac{1}{\omega} - \frac{1}{2})c_s^2 = (\tau - \frac{1}{2}\Delta t)c_s^2$. However, the simplicity has to pay the price of necessarily using square lattices of constant spacing (Δx=Δy) and consequently lead to the unity of the Courant-Fridrich-Levy (CFL) number due to $\Delta x = \Delta y = \Delta t$.

With the choice of viscosity in the above, Eq. (1) is formally a second order method (excluding the boundary conditions) for solving near-incompressible flows [6]. Physical and numerical constraints require that $\tau/\Delta t > 1/2$ or equivalently $\omega < 2$. In general, Eq. (1) is solved in two steps:

collision step:

$$f_i^*(\bar{x}, t+\Delta t) = f_i(\bar{x}, t) - \frac{1}{\tau}[f_i(\bar{x}, t) - f_i^{eq}(\bar{x}, t)] \quad (7a)$$

streaming step:

$$f_i(\bar{x} + \bar{e}_i\Delta t, t+\Delta t) = f_i^*(\bar{x}, t+\Delta t) \quad (7b)$$

which is known as the LBGK method [13]. Note that, in the above, * denotes the post- collision values. It is obvious that the collision process is completely localized, and the streaming step requires little computational effort by advancing the data from neighboring lattice points that makes Eq. (1) perfect for parallel implementation, which will be shown in detail later.

Previous experience in obtaining solutions at higher Reynolds numbers using SRT model of the LBE method has shown that the solution field (*u,v,p*) often exhibits spurious spatial oscillations in regions of large gradient such as stagnation point and sharp concave corners [10]. For example, it has shown that the serious spatial oscillations of pressure field can be clearly observed at Reynolds number of 5,000 with 256x256 lattice points at the upper two concave corners [10]. Depending upon the geometry and flow problem, such spatial oscillation may even propagate to contaminate the flow solutions in the regions far away from the singular points. In addition, the spatial oscillations in the solution can strongly affect the computational stability and convergence rate. Of course, the LBE using SRT model can always improve its computational stability and convergence by increasing the number of lattice points in the computational domain, although it is not recommended in general. Therefore, to develop a similar LBE technique but simple enough in implementation is strongly required to resolve the above-mentioned deficiencies.

II.2 Lattice Boltzmann Method with MRT model

Recently, Lallemand and Luo [12] suggested that the use of a MRT model could improve the numerical stability and reduce dramatically the unphysical oscillations for some simple flows. They have performed detailed theoretical analysis on the dispersion, dissipation and stability characteristics of a generalized lattice Boltzmann equation model proposed by d'Humieres [6]. They have found that the MRT model is equivalent to the SRT model in the long wavelength (low wave number) limit for macroscopic variables of interest in various simple flows through the linearized analysis [12]. Difference between two relaxation models is identified as a high-order effect (short wavelength limit), which can hardly detected in simple flows. It is well known that geometrically and mathematically singular pointes can adversely affect the flow solution in short wavelength limit. We would thus expect, at least, the solution of MRT model near the singular point is appreciably different from that of SRT model. For convection-dominated flows, the local difference near the singularities may also lead to large differences in flow regimes far away. Thus, it is important to understand how the solution using MRT model is different from that using SRT model. In addition, it is potentially useful to compute flows at higher Reynolds numbers using MRT model in LBM. In what follows, we will briefly summarize the important features of MRT model [12] as compared with those of SRT model.

Lallemand and Luo [12] have defined a new column vector of macroscopic variables

$\overline{R} = (\rho, e, \varepsilon, j_x, q_x, j_y, q_y, p_{xx}, p_{xy})^T$ and $\overline{R}$ can be related to the column vector of $\overline{F} = (f_0, f_1, f_2, f_3, f_4, f_5, f_6, f_7, f_8)^T$ as follows,

$$\overline{R} = \begin{bmatrix} \rho \\ e \\ \varepsilon \\ j_x \\ q_x \\ j_y \\ q_y \\ p_{xx} \\ p_{xy} \end{bmatrix} = \begin{bmatrix} 1 & 1 & 1 & 1 & 1 & 1 & 1 & 1 & 1 \\ -4 & -1 & 2 & -1 & 2 & -1 & 2 & -1 & 2 \\ 4 & -2 & 1 & -2 & 1 & -2 & 1 & -2 & 1 \\ 0 & 1 & 1 & 0 & -1 & -1 & -1 & 0 & 1 \\ 0 & -2 & 1 & 0 & -1 & 2 & -1 & 0 & 1 \\ 0 & 0 & 1 & 1 & 1 & 0 & -1 & -1 & -1 \\ 0 & 0 & 1 & -2 & 1 & 0 & -1 & 2 & -1 \\ 0 & 1 & 0 & -1 & 0 & 1 & 0 & -1 & 0 \\ 0 & 0 & 1 & 0 & -1 & 0 & 1 & 0 & -1 \end{bmatrix} \begin{bmatrix} f_0 \\ f_1 \\ f_2 \\ f_3 \\ f_4 \\ f_5 \\ f_6 \\ f_7 \\ f_8 \end{bmatrix} = \overline{\overline{M}}\overline{F} \tag{8}$$

where $\overline{\overline{M}}$ is a 9x9 matrix transforming $\overline{F}$ to $\overline{R}$. In the column vector $\overline{R}$, ρ is the fluid density, ε is related to the square of the energy e, j_x and j_y are the mass flux in two directions, q_x and q_y correspond to the energy flux in two directions, and p_{xx} and p_{xy} correspond to the diagonal and off-diagonal component of the viscous stress tensor. One immediate advantage of the MRT model is that macroscopic variables of interest can be obtained readily by simply performing the matrix multiplication $\overline{\overline{M}}\overline{F}$ if $\overline{F}$ is known. In addition, due to the conservation of mass and momentum before and after particle collision, the total mass and momentum should not relax at all. However, Eq. (7a) in standard LBGK method requires all f_i's are relaxed at the same rate and, hence, all macroscopic quantities of interest. Physically speaking, different physical modes should have different relaxation rates. By taking this into account in the MRT model, based on Eq. (7a), the collision procedure for $\overline{R}^*$ is performed as follows,

$$\overline{R}^* = \begin{Bmatrix} \rho^* = \rho - s_1(\rho - \rho^{eq}) \\ e^* = e - s_2(e - e^{eq}) \\ \varepsilon^* = \varepsilon - s_3(\varepsilon - \varepsilon^{eq}) \\ j_x^* = j_x - s_4(j_x - j_x^{eq}) \\ q_x^* = q_x - s_5(q_x - q_x^{eq}) \\ j_y^* = j_y - s_6(j_y - j_y^{eq}) \\ q_y^* = q_y - s_7(q_y - q_y^{eq}) \\ p_{xx}^* = p_{xx} - s_8(p_{xx} - p_{xx}^{eq}) \\ p_{xy}^* = p_{xy} - s_9(p_{xy} - p_{xy}^{eq}) \end{Bmatrix} = \overline{R} - \overline{\overline{S}}(\overline{R} - \overline{R}^{eq}) \tag{9}$$

where * denotes the post-collision state, $\overline{\overline{S}}$ is the 9x9 diagonal matrix, which will be shown later. In $\overline{\overline{S}}$, s_1=s_4=s_6=0 enforces mass and momentum conservation before and after collision. Note that the equilibrium values in $\overline{R}^*$ can be written as [12]

$$\begin{cases} e^{eq} = -2\rho + 3(u^2 + v^2) \\ \varepsilon^{eq} = \rho - 3(u^2 + v^2) \\ q_x^{eq} = -u \\ q_y^{eq} = -v \\ p_{xx}^{eq} = u^2 - v^2 \\ p_{xy}^{eq} = uv \end{cases} \tag{10}$$

Before the streaming step, Eq. (7b), is performed, one needs to transform the post-collision values, $\overline{R}^*$, back to $\overline{F}^*$ by using Eq. (9),

$$\overline{F}^* = \overline{\overline{M}}^{-1}\overline{R}^* = \overline{F} - \overline{\overline{M}}^{-1}\overline{\overline{S}}(\overline{R} - \overline{R}^{eq}) \tag{11}$$

where $\overline{\overline{S}}$ is the diagonal matrix,

$$\overline{\overline{S}} = \begin{bmatrix} 0 & 0 & 0 & 0 & 0 & 0 & 0 & 0 & 0 \\ 0 & s_2 & 0 & 0 & 0 & 0 & 0 & 0 & 0 \\ 0 & 0 & s_3 & 0 & 0 & 0 & 0 & 0 & 0 \\ 0 & 0 & 0 & 0 & 0 & 0 & 0 & 0 & 0 \\ 0 & 0 & 0 & 0 & s_5 & 0 & 0 & 0 & 0 \\ 0 & 0 & 0 & 0 & 0 & 0 & 0 & 0 & 0 \\ 0 & 0 & 0 & 0 & 0 & 0 & s_7 & 0 & 0 \\ 0 & 0 & 0 & 0 & 0 & 0 & 0 & s_8 & 0 \\ 0 & 0 & 0 & 0 & 0 & 0 & 0 & 0 & s_9 \end{bmatrix} \tag{12}$$

Finally, the streaming step for all f_i's in the MRT model is performed exactly the same as in the standard LBGK model using Eq. (7b).

Lallemand and Luo [12] have shown that the MRT model can reproduce the same viscosity as that by SRT model if we set $s_8 = s_9 = 1/\tau$. Once this is decided, the rest of the relaxation parameters (s_2, s_3, s_5 and s_7) for different physical modes can then be chosen more flexibly. In Ref. 12, they recommended the values to be slightly greater than unity. In this research, we will make some sensitivity study of these parameters in the current test case to see if complicated flow has different optimum values. Finally, it is worthy to note that the MRT model reduces to the SRT model by simply setting

$s_2 = s_3 = s_5 = s_7 = s_8 = s_9 = 1/\tau$.

II.3 Boundary conditions

Stationary Wall Boundary Conditions

How to properly implement the wall boundary conditions within LBM framework is still an ongoing research topic [14] and reference cited therein. The most often-used scheme is the so-called "bounce back" scheme, which has been argued that it is only of first-order accuracy as compared with of second-order accuracy for LBM formulation. However, it was recently shown that the error is sufficiently small if the relaxation parameter ω (or 1/τ) is chosen to be close enough to 2 [14]. Thus, we believe that the bounce-back boundary conditions in the current study shall not influence the order of accuracy of LBM using SRT and MRT models if we choose ω to be within some range.

Moving Wall Boundary Conditions

For the current problem, we have assumed equilibrium distribution function at the upper moving plate, which is computed by substituting the uniform plate velocity into Eq. (2) and the initial density assignment. After streaming, the velocity at the top plate is reinforced to be the uniform plate velocity and then the equilibrium distribution function is reevaluated using the fixed plate velocity and the updated density at the plate. In the current study, the upper two corner lattice points are considered as the part of the moving plate. The uniform top plate velocity is U=0.1, considering the validity of using LBM in simulating near-incompressible flows.

III. RESULTS AND DISCUSSIONS

To clearly demonstrate and test the advantages of LBM using MRT model over that using SRT model, we compute a steady, upper lid-driven flow (Re=100-7,500) by LBM using both MRT and SRT models. We compare various macroscopic variables of interest in regions of both large and small gradients. In addition, results from the LBM using MRT and SRT models are compared with those of N-S solvers by Ghia *et al*. [15] where it is appropriate.

Fig. 2 demonstrates the typical test of grid sensitivity (64x64 and 256x256 lattice points) by comparing the velocity profiles (Re=1,000) at the centerline of the cavity for both SRT and MRT models with the data by Ghia *et al.* [15], which has been considered to be the most comprehensive computation for the impressible lid-driven cavity flow. It is clearly shown that the difference of velocity distributions between the current study and Ghia *et al.* [15] is very small at 256x256 lattice points. Also the difference between MRT and SRT models is nearly undistinguished at this Reynolds number of 1,000. Similar trends are found for other Reynolds numbers up to 7500 for both MRT and SRT models. Thus, all results discussed in the followings are computed using 256x256 lattice points, unless otherwise specified.

Fig. 3 shows the simulated velocity vectors for Reynolds number of 7500 for both SRT and MRT models. Note that only MRT model is able to predict the fourth minor vortex in the lower right-hand corner, which is also a geometrically singular point, while SRT model fails to predict the fourth minor vortex at this corner.

Simulated location (x- and y-coordinate) of major central vortex as a function of Reynolds numbers by both SRT and MRT models along with previous data by Ghia *et al.* [15] using is illustrated in Fig. 4. The results of the present work and that of Ghia *et al.* [15] are in excellent agreement within 0.8% for all Reynolds numbers, except for Re=2000, where the data is provided by Ghia *et al.* [15]. In addition, excellent agreement between STR and MRT models is also found.

Fig. 5 shows the vorticity distribution using both SRT and MRT models at Re=7,500. It is clear that the vorticity distribution using these two models is approximately the same for Re=100, 400, 1000 and 2000. However, for Re=7,500 (similarly for Re=5,000), there exists obvious vorticity "jiggles" around the upper two cavity corners using SRT model, especially the left-hand one due to the geometrical singularity at this corner.

The above-mentioned differences for SRT and MRT models are highlighted again more clearly by the pressure contours at various Reynolds numbers as shown in Fig. 6. The pressure deviation is defined as $c_s^2 \times (\rho - \overline{\rho})$, where $\overline{\rho}$ is the average fluid density of within

the cavity. In these figures, values of pressure deviation are multiplied by 1,000 for the purpose of illustration clarity. The situation becomes worse even in regions far away from the corner at Re=7,500 for SRT model, while the pressure contour remains normal at this Reynolds number for MRT model.

Fig. 7 illustrates the comparison of u and v velocity distributions very close to the left vertical wall (i=2 lattice point) for SRT and MRT models at RE=7,500. Results clearly show that the velocity distributions (both u- and v-velocity) by SRT model present obvious spatial oscillations close to the upper-left corner, while the velocity distributions by MRT model present much less spatial oscillation in the same region of interest. In general, the spatial oscillation of solution around the upper-left corner becomes worse as Reynolds number increases. The difference represents that MRT model is more suitable, as compared with SRT model, for treating flow around geometrical singularity and potentially higher Reynolds-number flows, at least, for steady flows.

Finally, sensitivity of selecting the relaxation parameters (s_2, s_3, s_5 and s_7) has shown (Fig. 8 for RE=1000, 64x64 lattice points) to be relatively small once their values are close to 1.1. For values of the relaxation parameters close to 1.9, the spatial oscillations of the u- and v-velocity appear to be serious. Also the deviation increases with increasing Reynolds number as expected. Note that for the results presented in the above, they are all set to 1.1 for the simplicity, unless otherwise specified.

IV. CONCLUSIONS

In the current study, an upper, lid-driven cavity flow is simulated by parallel lattice Boltzmann method using multi-relaxation time scheme. Results are then compared with those by LBM using single-relaxation time scheme and previous published data using N-S solver. In general, results using MRT and SRT techniques are both in good agreement with those using N-S solver for Re=100-7500 for the most part of the flow within the cavity. In summary, we can conclude that MRT technique is superior to SRT technique in simulating higher Reynolds number flows having geometrical singularity with much less spatial oscillations due to the different relaxation rates for different physical modes embedded in the MRT scheme. In addition, the code using the MRT model takes only about 15% more CPU time than that using SRT model. Test for unsteady (periodic) flow, e.g., a flow past an obstacle with votex shedding using MRT technique is currently in progress and will be reported in the near future.

REFERENCES

1. Higuera, F.J. and Jeminez, J., "Boltzmann approach to lattice gas simulations," Europhysics Letter, Vol. 9, 1989; pp. 663-668.
2. Higuera, F.J., Succi, S. and Benzi, R., "Lattice gas-dynamics with enhanced collisions, Europhysics Letter, Vol. 9, 1989; pp. 345-349.
3. Bhatnagar, P.L., Gross, E.P. and Krook, M., "A model for collision proceses in gases. I. Small amplitude processses in charged and neutral pn-component system," Physical Review, Vol. 94, 1954; pp. 511-525.
4. Chen, H., Chen, S. and Matthaeus, W.H., "Recovery of the Navier-Stokes equations using a lattice Boltzmann method," Physical Review A, Vol. 45, 1992; pp. R5339-R5342.
5. Kandhai, D., Koponen, A., Hoekstra, A., Kataja, M., Timonen, J. and Sloot, P.M.A., "Lattice Boltzmann hydrodynamics on parallel systems," Computer Physics Communications, Vol. 111, 1998; pp. 14-26.
6. Dieter A. Wolf-Gladrow, "Lattice Gas Cellular Automata and Lattice Boltzmann Models", Springer, 2000.
7. Krafczyk M., M. Schulz, E.Rank, " Lattice-gas simulatios of two-phase flow in porous media," Communicatios in Numerical Methods in Engineering, Vo. 14, 1998; pp. 7-12.
8. Kono, K., Ishizuka, T. and Tsuba, H., "Application of lattice Boltzmann model to multiphase flows with phase transition," Computer Physics Communications, Vol. 129, 2001; pp. 110-120.
9. Hashimoto, Y. and Ohashi, Y., "Droplet dynamics using the lattice-gas method," International Journal of Modern Physics C, Vol. 8, 1997; pp. 977-983.

10. Hou, S., Lattice Boltzmann Method for Incompressible, Viscous Flow. PhD Thesis, Department of Mechanical Engineering, Kansas State University, 1995.
11. D'Humieres, D., "Generalized lattice Boltzmann equation, in Rarefied Gas Dynamics: Theory and Simulations, Progress in Astronautics and Aeronautics, Vol. 159, edited by Shizgal, B.D. and Weaver, D.P., AIAA, Washington, D.C., 1992; pp. 45-458.
12. Lallemand, P. and Luo, L.-S., "Theory of the lattice Boltzmann method: dispersion, dissipation, isotropy, Galilean invariance, and stability," Phys. Rev. E., Vol. 61, 2000; pp. 6546-6562.
13. Chen, S. and Doolen, G.D., "Lattice Boltzmann method for fluid flows," Ann. Rev. Fluid Mech., Vol. 30, 1998; pp. 329-364.
14. Inamuro, T., Yoshine, M. and Ogino, F., "A non-slip boundary condition for lattice-Boltzmann simulations," Phys. Fluids, Vol. 7, 1995; pp. 2928-2930.
15. U Ghia, K. N. GHIA, and C. T. SHIN, " High-Re solutions for incompressible flow using the Navier-Stokes equations and a multigrid method," Journal of Computational Physics 48, 1982; pp.387-411

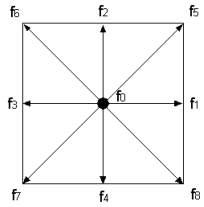

Fig. 1 D2Q9 model

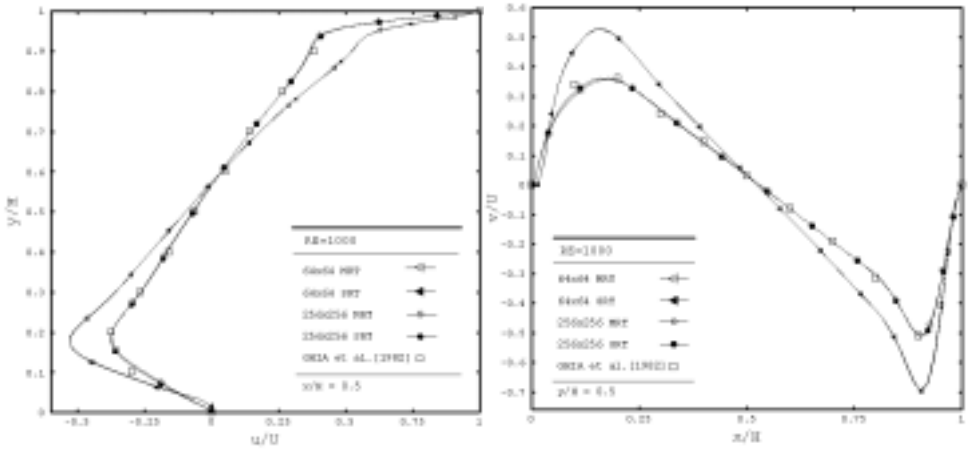

Fig. 2 Velocity profiles for u, v along the geometric centerline of the cavity

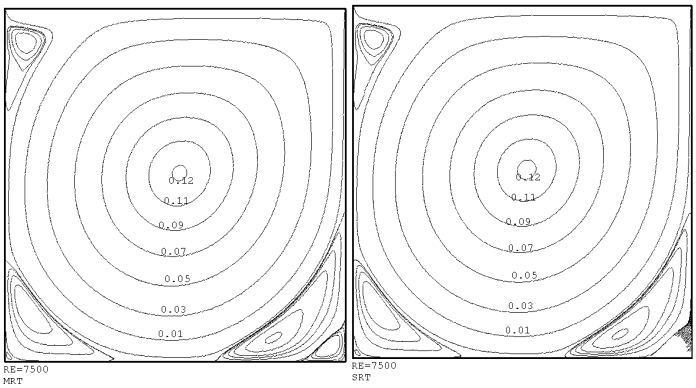

Fig.3 Streamline plot at Re=7500

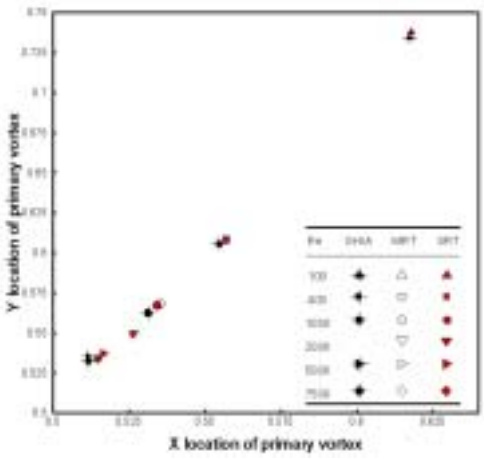

Fig.4 The location of the center of the primary vortex for different values of Reynolds, SRT and MRT models

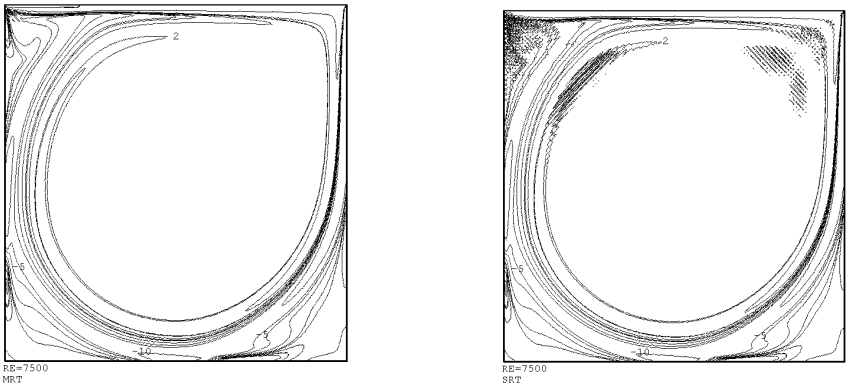

Fig. 5 Contour plots of vorticity at Re=7,500

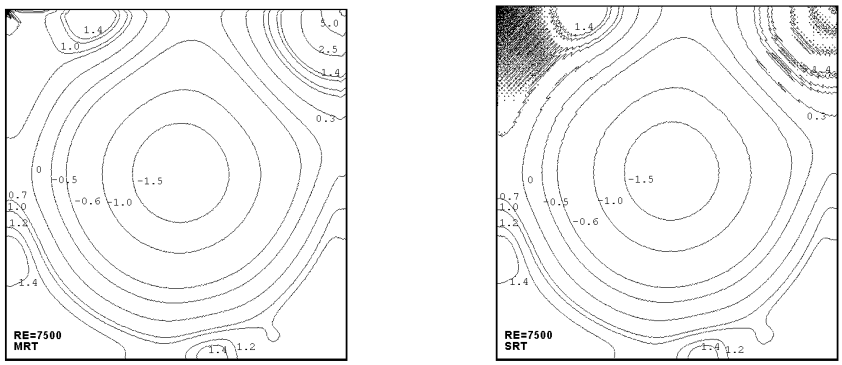

Fig.6 Normalized pressure contours at Re=7,500

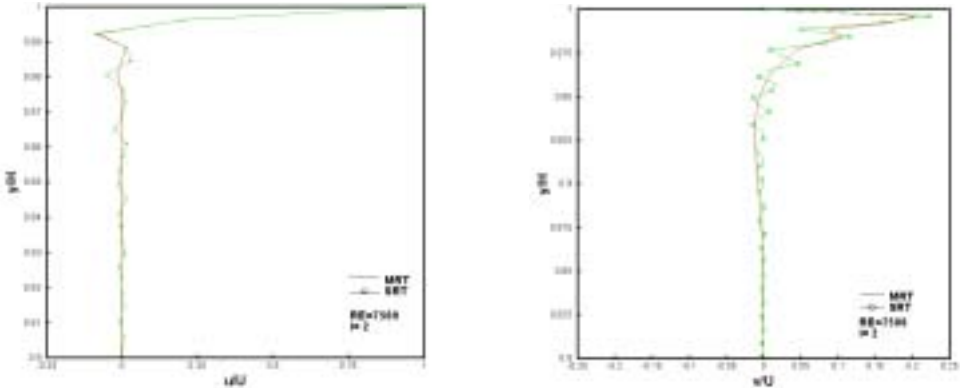

Fig. 7 Comparison of the velocity profiles at Re=7,500 (i=2)

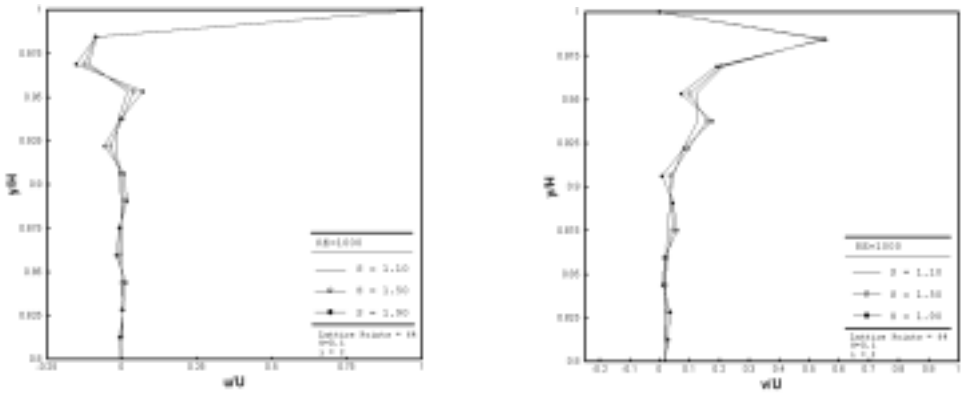

Fig. 8 Sensitivity of the selecting relaxation parameters of the velocity profiles at i=2, Re=1,000